



**HAL**  
open science

# Effects of polystyrene on morphology and electrical performance of solution-processed thermally activated delayed fluorescent organic light-emitting diodes

Jonghyun Choi, Seungwon Lee, Mamatimin Abbas, Laurence Vignau,  
Byeong-Kwon Ju

## ► To cite this version:

Jonghyun Choi, Seungwon Lee, Mamatimin Abbas, Laurence Vignau, Byeong-Kwon Ju. Effects of polystyrene on morphology and electrical performance of solution-processed thermally activated delayed fluorescent organic light-emitting diodes. *Current Applied Physics*, 2023, 45, pp.25-29. 10.1016/j.cap.2022.10.010 . hal-04272618

**HAL Id: hal-04272618**

**<https://hal.science/hal-04272618v1>**

Submitted on 6 Nov 2023

**HAL** is a multi-disciplinary open access archive for the deposit and dissemination of scientific research documents, whether they are published or not. The documents may come from teaching and research institutions in France or abroad, or from public or private research centers.

L'archive ouverte pluridisciplinaire **HAL**, est destinée au dépôt et à la diffusion de documents scientifiques de niveau recherche, publiés ou non, émanant des établissements d'enseignement et de recherche français ou étrangers, des laboratoires publics ou privés.

Public Domain

# **Effects of polystyrene on morphology and electrical performance of solution-processed thermally activated delayed fluorescent organic light-emitting diodes**

Jonghyun Choi<sup>a,b</sup>, Seungwon Lee<sup>b</sup>, , Mamatimin Abbas<sup>a\*</sup>, Laurence Vignau<sup>a\*</sup>, Byeong-Kwon Ju<sup>b\*</sup>

<sup>a</sup>Laboratoire IMS

Université de Bordeaux, CNRS

Bordeaux INP, UMR 5218,

F-33607 Pessac, France

E-mail: [mamatimin.abbas@ims-bordeaux.fr](mailto:mamatimin.abbas@ims-bordeaux.fr)

E-mail: [laurence.vignau@ims-bordeaux.fr](mailto:laurence.vignau@ims-bordeaux.fr)

<sup>b</sup>School of Electrical Engineering

Korea University

Seoul 02841, South Korea

E-mail: [bkju@korea.ac.kr](mailto:bkju@korea.ac.kr)

\*Corresponding authors

E-mail address: mamatimin.abbas@ims-bordeaux.fr (M. Abbas) laurence.vignau@ims-bordeaux.fr (V. Laurence) bkju@korea.ac.kr (B.K. Ju)

## **Abstract**

A polymer was added to the emissive-layer (EML) solution of thermally activated delayed fluorescence organic light-emitting diodes (TADF-OLEDs) to enhance their electrical and optical performances. A blue 4CzFCN TADF emitter and m-CBP host were used with 15 wt% dopant, and 1 wt% polystyrene (PS) was added to this EML solution. The PS enhanced the surface morphology, electroluminescence (EL), and external quantum efficiency (EQE). Energy transfer between the host and the dopant material was verified by analyzing the photoluminescence and time-resolved photoluminescence. After PS treatment, the surface roughness was reduced, according to the root-mean-square value obtained using atomic force microscopy. Finally, we fabricated solution-processed TADF-based OLEDs with an EQE of 4.7% at 7.7 V and a maximum luminance of 3700 cd/m<sup>2</sup> at 10 V.

Keywords: thermally activated delayed fluorescence (TADF); organic light-emitting diodes (OLEDs); TADF OLEDs; polystyrene; polymer blend; surface morphology;

## **1. Introduction**

In April 2013, thermally activated delayed fluorescence (TADF)-based organic light-emitting diodes (OLEDs) were discovered by Adachi et al., and they have since attracted tremendous attention in academia and industry for use in displays because of their ability to achieve 100% internal quantum efficiency without heavy-metal complexes [1 - 5]. In general, intentionally induced steric-hindered TADF emitter molecules make their molecules enabling their singlet and triplet energy difference ( $\Delta E_{ST}$ ) to be less than 25.6 eV [6]. This amount of energy can be activated at room temperature, and at the same time, energy transfer happens from the triplet excitation state to the singlet excited state, which is called reverse intersystem crossing (RISC). In this way, 100% internal quantum efficiency could realize by emitting delayed fluorescence [7].

However, TADF-based OLEDs have drawbacks. In the case of a high concentration of dopant molecules in the emissive layer (EML), the photoluminescence (PL) quantum yield decreases significantly because of self-quenching among the dopant materials due to intermolecular energy transfer (IET) [8]. However, IET between the host and dopant molecules, as well as both Dexter and Forster resonance energy transfers, are crucial for optimizing the electrical performance of TADF-based OLEDs [9].

Solution-processed OLEDs have various advantages, such as high reproducibility, large-area applicability, and simple fabrication processes. However, the solution process presents challenges, such as the poor film morphology and non-uniform crystallization during spin-coating [2-5,10-11]. It causes severe intermolecular aggregation between emitter molecules. In this study, 4CzFCN TADF emitter underwent that aggregation, and this led to degradation of its performance as an emitting material. Therefore, attempts have been made to enhance the film morphology and device performance by using a hybrid host comprising a polymer

and small molecules [12] and by introducing a polymer into the EML in polymer light-emitting diodes [13]. Electrically “inert” polystyrene (PS), which is known to suppress the formation of interchain interactions, was used in ~~the~~ this study [13-14]. Several groups have reported that supramolecular complexes can be formed in the atmosphere of small organic molecules only by adding a polymer such as a polystyrene. It could in turn lead to improved solubility, and the ability to form a homogeneous film for setting up large-scale optoelectronic devices [15 - 18].

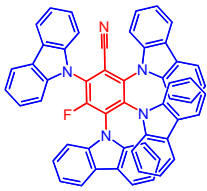
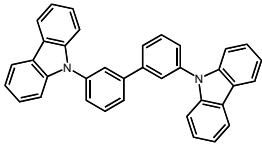
## 2. Experimental Details

15 mm × 15 mm ITO (170 nm, 10 Ω/sq) glasses purchased from Visiotek System Ltd. were used as substrates. A Hellmanex™ detergent solution was used to clean the substrates for 15 min at 60 °C to remove all the organic and inorganic residues. To remove the detergent solution, the substrates were sonicated with deionized water three times (for 5 min each) to rinse and cleaned with acetone, ethanol, and isopropanol for 15 min each. Subsequently, they were exposed to UV-ozone for 20 min to enhance the hydrophilic nature of the surface and eliminate residual organic compounds.

PH1000 poly(3,4-ethylenedioxythiophene) polystyrene sulfonate (PEDOT:PSS) was purchased from Heraeus. Owing to its high conductivity and optical transparency, PH1000 PEDOT:PSS was utilized as the hole-transport layer (HTL) in this study. A TADF blue emitter 4CzFCN (2,3,4,6-tetra(9H-carbazol-9-yl)-5-fluorobenzonitrile) and a TADF-OLED host m-CBP (3,3'-di(9H-carbazole-9-yl)biphenyl) were used as EML materials, as shown in Table 1, and were purchased from Lumtec Corp., Taiwan. Soluble blue TADF emitter was designed to enhance the solubility and pure blue emission. The F atom was incorporated into the molecular design because of its hydrophobic nature and relatively weak electron-

withdrawing property, whereas the four carbazole functional groups functioned as electron donors [9]. In addition, meta-linked m-CBP is a promising host candidate owing to its hole-transport properties and high triplet energy (2.8 eV), resulting in a high electron current density and external quantum efficiency (EQE) [19]. Therefore, 4CzFCN and m-CBP were used as the host and dopant materials, respectively. Polystyrene (PS) with an average molar weight of 700,000 g/mol was purchased from Pressure Chemicals. Other undescribed chemicals were obtained from Sigma–Aldrich and used as received.

**Table 1. Electrical and chemical properties of the dopant (4CzFCN) and host (m-CBP) materials.**

	Dopant (TADF emitter)	Host
Chemical Structure		
Name (molecular formula)	4CzFCN (C <sub>55</sub> H <sub>32</sub> FN <sub>5</sub> )	m-CBP (C <sub>36</sub> H <sub>24</sub> N <sub>2</sub> )
Molecular Weight	781.87 g/mol	484.59 g/mol
LUMO/ HOMO	3.49 eV / 6.31 eV	2.7 eV / 6.1 eV
$\Delta E_{st}$	0.06 eV	-

The widely used fluorescent host material 2,2',2''-(1,3,5-benzinetriyl)-tris(1-phenyl-1-H-benzimidazole) (TPBi) was used as the electron-transport and hole-blocking layer in the

device, simultaneously. Its shallow lowest unoccupied molecular orbital (LUMO) energy level (2.7 eV) makes it an excellent electron-transport material, while its deep highest occupied molecular orbital (HOMO) energy level (6.7 eV) provides a hole-blocking ability [20]. Ultrathin lithium fluoride (LiF) films exhibit electron-injection properties because they reduce the work function of Al, as measured by Shaheen et al. [21]. In this study, the doping concentration of 4CzFCN in m-CBP was fixed at 15 wt% after several trials for determining the optimal conditions. Likewise, chlorobenzene was selected among several solvents, such as chloroform and toluene. The concentration of the EML solution was fixed at 10 mg/mL.

A filtered (Sartorius Minisart RC Syringe Filters, 0.2  $\mu\text{m}$ ) PEDOT:PSS (PH1000) solution was prepared for spin-coating at 4000 rpm for 60 s to obtain a 40-nm HTL, which was measured using a Dektak surface profilometer. Next, the substrates were annealed at 120  $^{\circ}\text{C}$  for 10 min to evaporate the residual solvent. Then, a 40-nm-thick layer of m-CBP doped with 4CzFCN EML was spin-coated at 2000 rpm for 60 s from a chlorobenzene solution, followed by annealing at 100  $^{\circ}\text{C}$  for 10 min (for the same reason as before) under a nitrogen atmosphere in a glovebox. While maintaining a nitrogen environment, we thermally evaporated a 40-nm-thick TPBi layer (ETL), a 1-nm-thick LiF layer (EIL), and a 100-nm-thick Al layer (cathode) under high-vacuum conditions ( $10^{-6}$  mbar) at rates of 1.1, 0.4, and 12  $\text{\AA s}^{-1}$ , respectively.

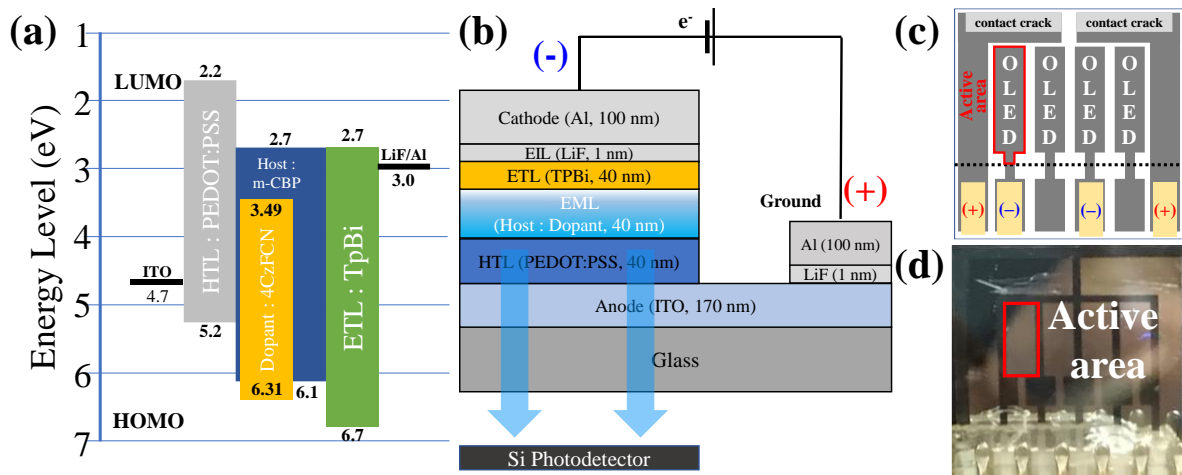


**Figure 1. (a) Band diagram of host–dopant mixed OLEDs; (b) schematic of the bottom-emission OLED device whose JVL characteristics were measured using a photo detector and probes (c) device schematic and (d) photograph showing the contact position.**

Figure 1 (a) shows a band diagram of the TADF OLEDs investigated in this study. Indium tin oxide (ITO)-doped glass was used as the substrate and anode, and PEDOT:PSS, 4CzFCN, m-CBP, TPBi, LiF, and Al were used as the HTL, dopant, host, electron-transport layer (ETL), electron-injection layer (EIL), and cathode, respectively. Figure 1 (b) shows a schematic of the bottom-emission OLED device, including the contact position and composition used for luminance measurements. The contact pad and active area of  $10.5 \text{ mm}^2$  are shown in Figure 1 (c) and (d), respectively. A solution-processed OLED was fabricated with the configuration ITO (170 nm)/PEDOT:PSS (40 nm)/m-CBP:4CzFCN (15 wt%, 40 nm)/LiF (1 nm)/Al (100 nm) as a bottom-emission OLED.

The current and voltage were measured using a program-controlled Keithley 4200 probe station. The luminance was measured from the luminance meter (Minolta CS-100) at a certain voltage, then by comparing luminance with the voltage converted from the



photocurrent of the photodetector amplifier (C9329), we calculated the luminance as a function of voltage. The current efficiency (CE) and power efficiency (PE) were calculated using the luminance, current, voltage, and area of the active layer.

The time-resolved photoluminescence (TRPL) spectra were measured using a Quantaaurus-Tau fluorescence lifetime measurement system (C11367-03) from Hamamatsu Photonics Co., and the prompt and delayed lifetimes were calculated using tau U11487 software.

The external quantum efficiency (EQE) was calculated as the number of photons driven out of the device divided by the number of electrons generated inside the device. A 3D-printed device was designed with a UV–vis spectrophotometer (Ocean Optics, HR2000) and a potentiostat (Keithley 4200) to measure the EL by applying a constant current. Using a reference white light-emitting diode (Thorlabs, model LEDSW30), we converted the EL spectrum into the number of photons.

### **3. Results and discussion**

The ultraviolet–visible (UV–vis) absorption and PL spectra of the dopant alone (4CzFCN), host alone (m-CBP), and host doped with the dopant (m-CBP:4CzFCN) shown in Figure 2 indicate whether energy was transferred from the host to the dopant material. The dopant alone, host alone, and dopant–host are represented by red, blue, and green colors, respectively. We observed peaks at 525, 420, and 475 nm. Owing to a slight energy transfer between the host and the dopant, the m-CBP:4CzFCN OLED had a PL emission peak between those of 4CzFCN and m-CBP. However, the energy transfer was not complete.

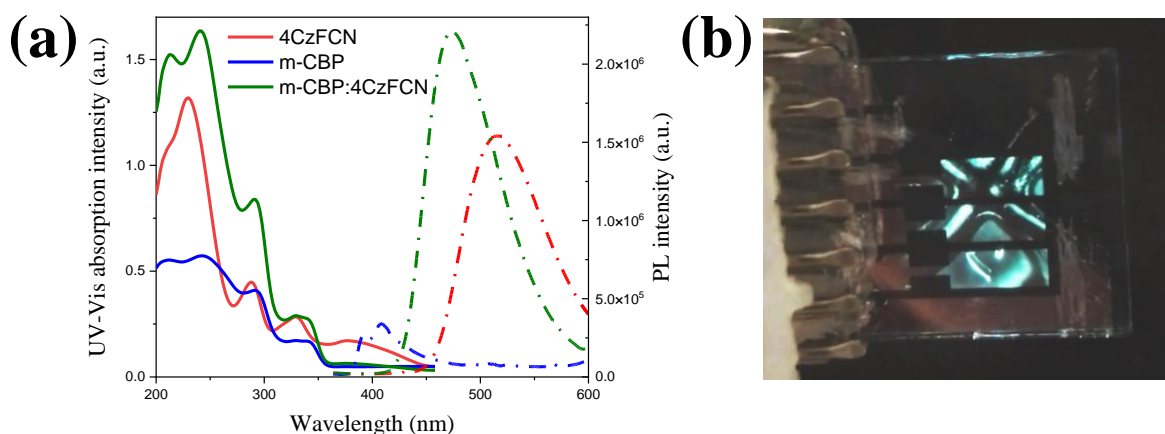


**Figure 2. (a) UV–vis absorption and PL emission spectra of the dopant, host, and host doped with dopant OLED device (red: 4CzFCN; blue: m-CBP; green: m-CBP:4CzFCN). The straight line corresponds to the absorption, and the dashed-dotted line corresponds to the PL emission spectra. (b) An operating picture of 4CzFCN:m-CBP OLED devices having a non-uniformly emitting area that is caused by spin-coating.**

Moreover, some of the devices had spin-coating issues, as shown in Figure 2 (b). A nonuniformly deposited EML layer was observed. In order to overcome this problem, an additional polymer was added to the active layer to improve the homogeneity of the film and to enhance the electroluminescence (EL) performance.

Polystyrene (PS) was selected as an additive polymer material because several studies have indicated that it enhances the performance of electrical devices, including OLEDs [13, 15-18] and thin-film transistors [22]. PS and EML solutions were prepared separately to ensure solubility in the solvent and were then mixed. We added 1 wt% PS to a 15 wt% m-CBP doped with 4CzFCN EML solution.

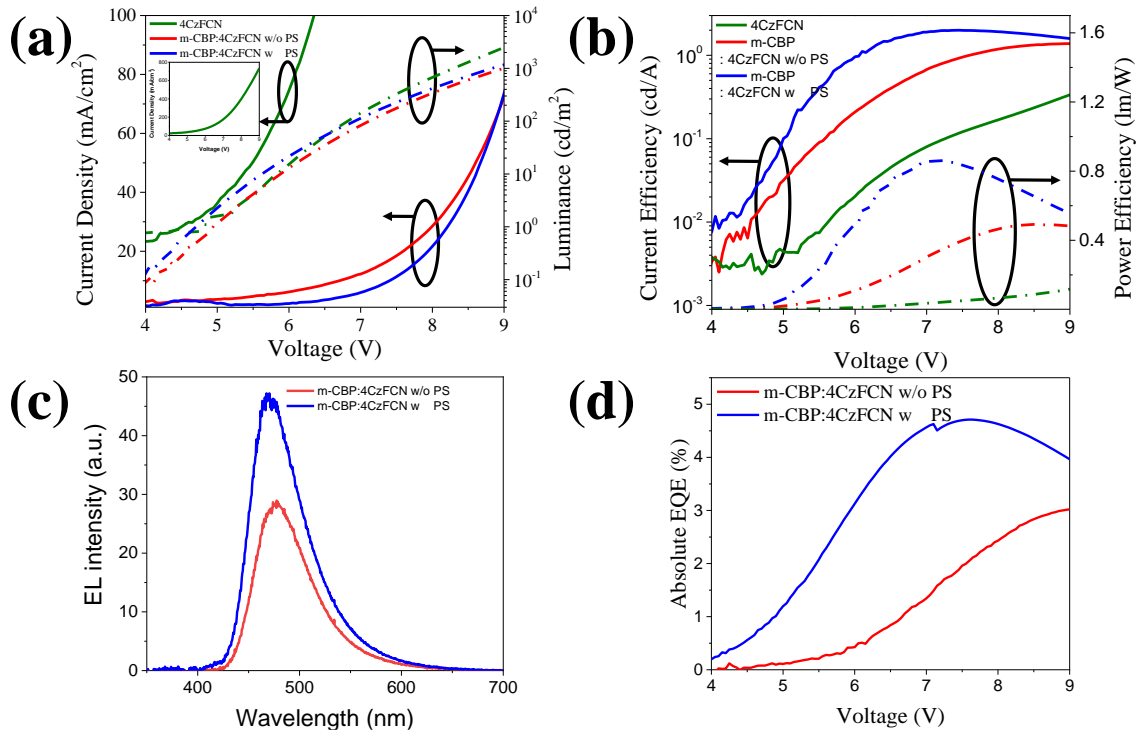


**Figure 3. Effects of PS addition on the characteristics of the OLED device: (a) JV L characteristics (inlet graph represents current density of 4CzFCN); (b) CE and P E; (c) EL; (d) absolute EQE characteristics (red: m-CBP doped with 4CzFCN with out PS; blue: m-CBP doped with 4CzFCN with PS; green: 4CzFCN OLED).**

The electrical characteristics of the OLED devices shown in Figure 3 include the JVL characteristics, current efficiency (CE), power efficiency (PE), EL, and EQE. Red, blue, and green correspond to 4CzFCN alone, m-CBP:4CzFCN without PS, and m-CBP:4CzFCN with PS, respectively. In the case of 4CzFCN alone, device degradation occurred at 9 V, whereas the other devices remained operational up to 11 V. As indicated by the JVL characteristics shown in Figure 3 (a), with regard to luminance, there were no significant differences among the three devices; however, the current density of the 4CzFCN-alone OLED device was more than seven times higher than those of the other two devices at 9 V. This is because, in host-dopant devices, exciton trapping and energy transfer from the host singlet and triplet to the

dopant singlet and triplet prevented the thermal degradation of the device. Additionally, the electron-hole pairs recombined more effectively with the host–dopant system [23].

Furthermore, the leakage current was lower than that of the dopant-alone OLED device.

The CE and PE results for the dopant-alone device were one order of magnitude lower than those for the host–dopant system, as shown in Figure 3 (b). The addition of PS hardly affected the efficiency, but it significantly improved the EL and EQE. Although the EL spectra of the devices shown in Figure 3 (c) with and without PS exhibited peaks at the same wavelength, the peak intensity was almost two times higher for the PS-added device. Figure 3 (d) shows the EQE with respect to the applied voltage; it was 4.7% at 7 V in the case of PS included and 2.9% at 9 V without PS. We assumed that the polymer-added EML solution formed a uniformly coated film, facilitating energy transfer and electron–hole recombination in the dopant–host system.

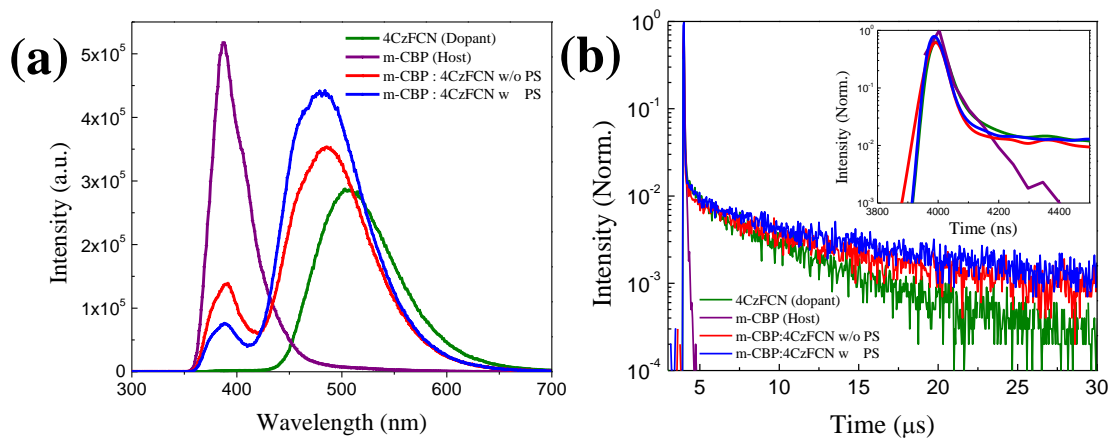


**Figure 4. (a) PL spectra; (b) TRPL of dopant alone, host alone, m-CBP:4CzFCN without and with PS OLED devices (inset presents prompt fluorescence in a nano second scale). Green, red, blue, and purple correspond to dopant alone, host alone, without PS, and with PS, respectively.**

The PL spectra of each device indicated nearly full the energy transfer from the host to the dopant, as shown in Figure 4 (a). The dopant and host exhibited peaks at 385 and 500 nm,

respectively. However, m-CBP doped with the 4CzFCN film exhibited two peaks from the dopant and host. Devices including PS exhibited a higher peak intensity from the dopant side (green) and a lower peak intensity from the host side (purple). This finding supports the hypothesis that PS facilitates intramolecular energy transfer.

**Table 2. Time-resolved fluorescence of the dopant, host, and host doped with dopant films:  $\tau_p$  (prompt fluorescence) and  $\tau_d$  (delayed fluorescence).**

active layer material	$\tau_p$	$\tau_d$
4CzFCN	10.5 ns	5.47 $\mu$ s
m-CBP	0.97 ns	0.077 $\mu$ s
m-CBP:4CzFCN (15 wt%) w/o PS	14.2 ns	11.67 $\mu$ s
m-CBP:4CzFCN (15 wt%) w PS	12.8 ns	13.79 $\mu$ s

Furthermore, the TRPL was analyzed to investigate the TADF effect, as shown in Figure 4 (b), as well as energy transfer. Because the host material was not a TADF material, the fluorescence emission of m-CBP decayed at the nanoscale, as expected. In contrast, 4CzFCN and m-CBP:4CzFCN exhibited prompt and delayed fluorescence emissions, respectively. By using tau U11487 software, PL and TRPL data were registered and calculated to obtain  $\tau_p$  (prompt fluorescence) and  $\tau_d$  (delayed fluorescence).

From the viewpoint of TADF, the dopant-alone device exhibited a delayed fluorescence

decay time of 5.47  $\mu\text{s}$ , and the devices without and with PS exhibited delayed decay fluorescence times of 11.68 and 13.79  $\mu\text{s}$ , respectively, as shown in Table 2. The dopant-alone device had the shortest delay time because the dopant concentration was relatively high; thus, triplet–triplet annihilation (TTA) frequently occurred [7]. The delayed fluorescence decay time was increased by helping the dopant and host material to be dispersed at regular intervals without agglomeration of the film uniformly deposited with PS.

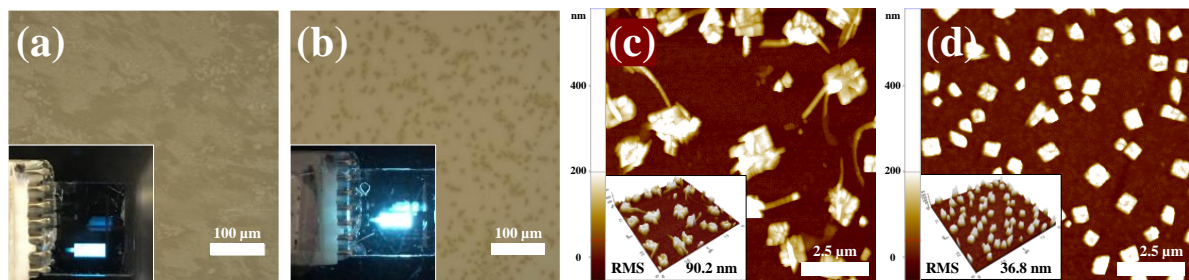


**Figure 5. Optical microscopy images of the EML (a) without PS and (b) with PS. AFM images of devices (c) without PS and (d) with PS.**

To confirm the effect of PS on the surface morphology, optical microscopy and atomic force microscopy were used. Figure 5 (a) and (b) show optical microscopy images of the devices without and with PS, respectively. From the optical images, we could not distinguish which device was better with regard to surface morphology; however, in the case of PS additive device appeared brighter to the bare eye, as shown in the insets of Figure 5 (a) and (b). Figure 5 (c) and (d) present AFM images of  $10\ \mu\text{m} \times 10\ \mu\text{m}$  areas. As shown, both devices had agglomerated particles on their surfaces. However, for the films mixed with PS, the sizes of the particles were significantly reduced, and the particles were evenly distributed. Additionally, the root-mean-square surface roughness value was reduced from 90.2 nm to 36.8 nm (almost by one-thirds). Even without taking into account large particles, the value of the root mean square is lowered from 15.4 nm to 12.0 nm. Therefore, these results naturally

demonstrated that PS can help evenly disperse emissive materials during the deposition of films.

## **6. Conclusion**

We fabricated a solution-processed TADF OLED with the following a structure of ITO/PEDOT:PSS/EML/TPBi/LiF/Al and investigated the effect of the dispersion of PS on its EL and EQE. A 4CzFCN dopant and m-CBP host were used in the EML layer. By comparing the PL spectra of the dopant alone, host alone, and dopant–host material-deposited films, we confirmed that energy transfer occurred between the host and dopant. In addition, a TRPL analysis indicated that the thermally activated delayed fluorescence phenomenon was due to the dopant material, and PS EML OLEDs exhibited the longest delay time (13.7  $\mu$ s) among the devices tested. This was mainly due to the homogeneously deposited EML film because the PS suppressed triplet-triplet annihilation (TTA) between the host and dopant materials.

Finally, regarding the surface morphology, a small amount of volume of PS was able to modify the surface. Therefore, the incorporation of PS helped to spread the emission material evenly, as indicated by the reduced surface roughness observed via AFM. Consequently, among the OLEDs tested, the brightest blue light was emitted from the PS-based OLED.

## **Acknowledgements**

This work was supported by Samsung Display Co.,Ltd.

## **Appendices**

Figure 1. (a) Band diagram of host–dopant mixed OLEDs; (b) schematic of the bottom-emission OLED device whose JVL characteristics were measured using a photodetector an



d probes (c) device schematic and (d) photograph showing the contact position.

Figure 2. (a) UV–vis absorption and PL emission spectra of the dopant, host, and host doped with dopant OLED device (red: 4CzFCN; blue: m-CBP; green: m-CBP:4CzFCN).

The straight line corresponds to the absorption, and the dashed-dotted line corresponds to the PL emission spectra. (b) An operating picture of 4CzFCN:m-CBP OLED devices having a non-uniformly emitting area that is caused by spin-coating.

Figure 3. Effects of PS addition on the characteristics of the OLED device: (a) JVL characteristics (inlet graph represents current density of 4CzFCN); (b) CE and PE; (c) EL; (d) absolute EQE characteristics (red: m-CBP doped with 4CzFCN without PS; blue: m-CBP doped with 4CzFCN with PS; green: 4CzFCN OLED).

Figure 4. (a) PL spectra; (b) TRPL of dopant alone, host alone, m-CBP:4CzFCN without and with PS OLED devices (inset presents prompt fluorescence in a nano second scale). Green, red, blue, and purple correspond to dopant alone, host alone, without PS, and with PS, respectively.

Figure 5. Optical microscopy images of the EML (a) without PS and (b) with PS. AFM images of devices (c) without PS and (d) with PS.

Table 1. Electrical and chemical properties of the dopant (4CzFCN) and host (m-CBP) materials.

Table 2. Time-resolved fluorescence of the dopant, host, and host doped with dopant films:  $\tau_p$  (prompt fluorescence) and  $\tau_d$  (delayed fluorescence).

## References

[1] H. Uoyama, K. Goushi, K. Shizu, H. Nomura, C. Adachi, Highly efficient organic light-emitting diodes from delayed fluorescence, *Nature* 492 (2012) 234–238. <https://doi.org/>

g/10.1038/nature11687

[2] Y.J. Cho, K.S. Yook, J.Y. Lee, High efficiency in a solution-processed thermally activated delayed-fluorescence device using a delayed-fluorescence emitting material with improved solubility, *Adv. Mater.* 26 (2014) 6642–6646. <https://doi.org/10.1002/adma.201402188>

[3] W. Jing, D. Song, B. Qiao, Z. Xu, J. Chen, L. Zhou, B. Li, S. Zhao, Managed carrier density and distribution in solution-processed emission layer to achieve highly efficient and bright blue organic light-emitting devices, *Org. Electron.* 82 (2020) 105703. <https://doi.org/10.1016/j.orgel.2020.105703>

[4] J. Hwang, C. Lee, J.-E. Jeong, C.Y. Kim, H.Y. Woo, S. Park, M.J. Cho, D.H. Choi, Rational design of carbazole-and carboline-based polymeric host materials for realizing high-efficiency solution-processed thermally activated delayed fluorescence organic light-emitting diode, *ACS Appl. Mater. Interfaces* 12 (2020) 8485–8494. <https://doi.org/10.1021/acami.9b20279>

[5] T.-W. Lee, T. Noh, H.-W. Shin, O. Kwon, J.-J. Park, B.-K. Choi, M.-S. Kim, D.W. Shin, Y.-R. Kim, Characteristics of solution-processed small-molecule organic films and light-emitting diodes compared with their vacuum-deposited counterparts, *Adv. Funct. Mater.* 19 (2009) 1625–1630. <https://doi.org/10.1002/adfm.200801045>

[6] Kim, B.S. and Lee, J.Y., 2014. Engineering of mixed host for high external quantum efficiency above 25% in green thermally activated delayed fluorescence device. *Adv. Funct. Mater.* 24 (2014) 3970-3977. <https://doi.org/10.1002/adfm.201303730>

[7] Godumala, M., Choi, S., Cho, M.J. and Choi, D.H., 2016. Thermally activated delayed fluorescence blue dopants and hosts: from the design strategy to organic light-emitting diode applications. *J. of Materials Chemistry C* 4 (2016) 11355-11381. <https://doi.org/10.1039/c6jm00000a>

039/C6TC04377A

[8] H.S. Kim, S.-R. Park, M.C. Suh, Concentration quenching behavior of thermally activated delayed fluorescence in a solid film, *J. Phys. Chem. C* 121 (2017) 13986–13997. <https://doi.org/10.1021/acs.jpcc.7b02369>

[9] H. Kang, H.J. Ahn, G.W. Kim, J.-E. Jeong, H.Y. Woo, J.-Y. Kim, and S. Park, Exciton energy transfer and bi-exciton annihilation in the emitting layers of thermally activated delayed fluorescence-based OLEDs, *J. Mater. Chem. C* 9 (2021) 15141–15149. <https://doi.org/10.1039/D1TC03626B>

[10] L. Duan, L. Hou, T.-W. Lee, J. Qiao, D. Zhang, G. Dong, L. Wang, Y. Qiu, Solution processable small molecules for organic light-emitting diodes, *J. Mater. Chem.* 20 (2010) 6392–6407. <https://doi.org/10.1039/B926348A>

[11] Y.J. Cho, B.D. Chin, S.K. Jeon, J.Y. Lee, 20% External quantum efficiency in solution-processed blue thermally activated delayed fluorescent devices, *Adv. Funct. Mater.* 25 (2015) 6786–6792.

[12] K.S. Yook, J.Y. Lee, Small molecule host materials for solution processed phosphorescent organic light-emitting diodes, *Adv. Mater.* 26 (2014) 4218–4233. <https://doi.org/10.1002/adfm.201502995>

[13] G. He, Y. Li, J. Liu, Y. Yang, Enhanced electroluminescence using polystyrene as a matrix, *Appl. Phys. Lett.* 80 (2002) 4247–4249. <https://doi.org/10.1063/1.1480098>

[14] E. Khodabakhshi, P.W.M. Blom, J.J. Michels, Efficiency enhancement of polyfluorene: Polystyrene blend light-emitting diodes by simultaneous trap dilution and  $\beta$ -phase formation, *Appl. Phys. Lett.* 114 (2019) 093301. <https://doi.org/10.1063/1.5058195>

[15] Singh, M., Haverinen, H.M., Dhagat, P. and Jabbour, G.E., Inkjet printing—process

and its applications. *Adv. Mater.* 22 (2010) 673-685. <https://doi.org/10.1002/adma.200901141>

[16] Lin, J.Y., Zhu, G.Y., Liu, B., Yu, M.N., Wang, X.H., Wang, L., Zhu, W.S., Xie, L.H., Xu, C.X., Wang, J.P. and Stavrinou, P.N., Supramolecular Polymer–Molecule Complexes as Gain Media for Ultraviolet Lasers. *ACS Mac. Lett.* 5 (2016) 967-971. <https://doi.org/10.1021/acsmacrolett.6b00394>

[17] Yan, X., Xu, D., Chi, X., Chen, J., Dong, S., Ding, X., Yu, Y. and Huang, F., A multiresponsive, shape-persistent, and elastic supramolecular polymer network gel constructed by orthogonal self-assembly. *Adv. Mater.* 24 (2012) 362-369. <https://doi.org/10.1002/adma.201103220>

[18] Sun, N., Han, Y., Sun, L., Xu, M., Wang, K., Lin, J., Sun, C., An, J., Wang, S., Wei, Q. and Zheng, Y., 2021. Diarylfluorene Flexible Pendant Functionalization of Polystyrene for Efficient and Stable Deep-Blue Polymer Light-Emitting Diodes. *Macromolecules.* 54 (2021) 6525-6533. <https://doi.org/10.1021/acs.macromol.0c02876>

[19] C.S. Oh, J.Y. Lee, C.H. Noh, S.H. Kim, Molecular design of host materials for high power efficiency in blue phosphorescent organic light-emitting diodes doped with an imidazole ligand based triplet emitter, *J. Mater. Chem. C* 4 (2016) 3792–3797. <https://doi.org/10.1039/C5TC02595H>

[20] C. Zou, Y. Liu, D.S. Ginger, L.Y. Lin, Suppressing efficiency roll-off at high current densities for ultra-bright green perovskite light-emitting diodes, *ACS Nano* 14 (2020) 6076–6086. <https://doi.org/10.1021/acsnano.0c01817>

[21] S.E. Shaheen, G.E. Jabbour, M.M. Morrell, Y. Kawabe, B. Kippelen, N. Peyghambarian, M.-F. Nabor, R. Schlaf, E.A. Mash, N.R. Armstrong, Bright blue organic light-emitting diode with improved color purity using a LiF/Al cathode, *J. Appl. Phys.* 84 (1998) 2

324–2327. <https://doi.org/10.1063/1.368299>

[22] M.M Hasan, M.M. Islam, X. Li, M. He, R. Manley, J. Chang, N. Zhelev, K. Mehrotra, J. Jang, Interface engineering with polystyrene for high-performance, low-voltage driven organic thin film transistor, *IEEE Trans. Electron Devices* 67 (2020) 1751–1756. <https://doi.org/10.1109/TED.2020.2974980>

[23] K. Xu, D. Ma, Electron–hole pair model in bulk-limited organic light-emitting diodes, *J. Phys. Chem. C* 119 (2015) 640–643. <https://doi.org/10.1021/jp508298j>